A quantitative risk assessment of waterborne infectious disease in the inundation area of a tropical monsoon region

So Kazama[a], Toshiki Aizawa[b], Toru Watanabe[a], Priyantha Ranjan[c], Luminda Gunawardhana[a]*, Ayako Amano[a]

[a] Department of Civil Engineering, Tohoku University, 6-6-06, Aramaki aza aoba, Aoba ku, Sendai, 980-8579, Japan

[b] Obayashi Corporation, Shinagawa Intercity Tower B, 2-15-2, Konan, Minato-ku, Tokyo, 108-8502, Japan

[c] Department of Civil Engineering, Curtin University, GPO Box U1987, Perth, WA 6845, Australia

* Corresponding author. Tel./fax: +81-22-795-7458

E-mail: luminda@kaigan.civil.tohoku.ac.jp , lumihg@yahoo.com

Abstract

Flooding and inundation are annual events that occur during the rainy season in Cambodia, and inundation has a strong relationship with human health. This study simulated the coliform bacteria distribution using a hydraulic model and estimated the impact of inundation on public health using a dose-response model. The model parameters were calibrated using field survey data from Cambodia and obtained good agreement with the coliform group count (CGC) distribution. The results suggest that the impact of inundation on human health is most noticeable in residential areas. The annual average risk of infection during medium-sized flood events is 0.21. The risk due to groundwater use ranges from 0.12 to 0.17 in inundation areas and reaches as high as 0.23 outside the inundation areas. The risk attributed to groundwater use is therefore higher than that for surface water use (0.02-0.06), except in densely populated areas at the city center. There is a high risk for infection with waterborne disease in residential areas, and the annual average risk during small flood events is 0.94. An assessment of possible countermeasures to reduce the risk shows that the control of inundation may bring more risk to public health in Cambodia. Shallower inundation water (< 0.3m) leads to a higher risk of infection, but if the depth is greater than 2m, the risk is low in residential areas. The simulated results explain the spatial distributions of infection risk that is vitally important for determining the highest priority places with relatively high risk and will be helpful for decision makers when considering the implementation of countermeasures.

Keywords: The Mekong River, Concentration of coliform bacteria, Dose-response model, Hydrological model

1. Introduction

Most monsoon regions, which are located downstream of continental rivers, face seasonal flood disasters (e.g., Cambodia and Vietnam from the Mekong River, Bangladesh from the Brahmaputra River, and Brazil from the Amazon River). Although these floods bring many benefits to the local people and ecosystem (Kazama et al. 2003; 2007), developing countries often suffer from social and economic damage due to inundation. Flooding is the leading cause of water-related mortality in most of these areas. In particular, regions without clean water supplies and proper sewage systems that must depend on surface and sub-surface water polluted by inundation have serious problems with waterborne infectious diseases. In addition, flooding can result in vector-associated problems, including increases in mosquito populations that, under certain circumstances, increase the risk for mosquito-borne infectious diseases (e.g., viral encephalitis). The public health impacts of floods also include damage or destruction to homes and the displacement of the occupants; these factors may, in turn, facilitate the spread of infectious diseases because of crowded living conditions and compromised personal hygiene. The multiple environmental consequences of flooding can directly affect the public's health. For example, water sources can become contaminated with fecal material or toxic chemicals, water or sewer systems can be disrupted, dangerous substances can be released, and solid-waste collection and disposal can be disrupted.

There are four billion cases of diarrhea each year in addition to millions of other cases of illness associated with the lack of access to clean water (WHO, 2000), and more than 5 million people die worldwide (Hunter et al., 2001). About 75% of the infectious disease cases are reported in tropical areas, and about 50% of the deaths (4,800 thousand people) occur in children under 5 years of age. Waterborne infectious disease takes hold in inundated areas during the flooding season. It is known that the flooded water distributes pollutants and contaminated matter from sumps (Smith 2001), and this commonly occurs in developing countries, increasing waterborne infectious disease. Epidemics of diarrhea during flooding were reported in Sudan, Mozambique, and India in 1980, 2000, and 1998, respectively (WHO 2005b). Schwartz et al. (2006) also reported clinical data for flood-associated diarrhea epidemics in Bangladesh.

Numerous attempts have been made by researchers to evaluate the risk of waterborne infectious disease due to floods. Currieto et al. (2001) conducted a quantitative analysis of the relationship between waterborne disease and heavy rainfall in US over a long-term period, and mentioned its obvious association with watersheds. Kunii et al. (2002) evaluated the health conditions of residents during a flooding episode in Bangladesh using public questionnaires. Muirhead et al. (2004) studied the relationship between *E. coli* concentration and water level and turbidity. Lloyd and Bartram (1991) evaluated the risk by looking at the combination of *E. coli* pollution of water resources and an environmental index. Information about the dose-response relationship is useful for evaluating the risk of infection. Lopez-Pila and Szewzyk (2000) determined this relationship for rotavirus in humans and evaluated the risk of infection in surface water. Climate change increases rainfall and inundation leading to waterborne disease outbreaks (Rose et al. 2000; Haines et al. 2006). However, no studies have tried to assess the risk of waterborne infectious disease due to flood in a continuous spatial-temporal movement.

The Mekong River is one of the largest inundation areas in a tropical monsoon region, and its basin spreads over six Asian countries. Severe floods have disastrous impacts and cause wide-ranging destruction downstream of the Mekong River basin, especially in Vietnam and Cambodia. In addition to the damage and destruction to infrastructure and the displacement of residents, floods mainly affect the public health by spreading infectious diseases in these regions. Therefore, evaluations and assessments of the effects of flooding on the spread of waterborne infectious disease and possible countermeasures are very important in this area. Cambodia has huge inundation areas which lead to difficulties for field observations. Therefore, an integrated risk evaluation of waterborne infectious diseases, using numerical simulations coupled with field observations, has been requested to understand the spatial and temporal distribution of waterborne infectious diseases.

In the recent literature regarding flood and inundation analysis in the Mekong delta, analyses have been carried out using various numerical methods (Inoue et al. 2000; Herath and Dutta 2000; Huu-toi and Gupta 2001). Most of these studies have focused on the lower part of Mekong river in Vietnam. The lack of available data for the Cambodian part of the Mekong River has resulted in fewer studies. Even though water resources and development plans aim to control the annual floods to reduce the inundation areas and flood damage in the Mekong Delta, no studies have been carried out to evaluate the effects of such measures and how changes in the inundation areas would affect the community and public health. The objective of the current study is to develop a numerical model expressing the coliform bacteria distribution by combining hydraulic models and models for the concentration of coliform bacteria. The risk is estimated from the numerical and dose-response models to determine the effects of floods of different magnitudes on different water sources. As flood-related public health problems were expected to continue into the recovery phase of the disaster, we performed an initial rapid public health assessment and established surveillance to monitor ongoing or anticipated flood-related health problems to ensure the detection of possible waterborne infectious disease outbreaks and flood-related injuries.

2. Study area

2.1. Lower Mekong River

The Mekong River has a length of approximately 4,900 km making it the world's 10th longest river (Liu et al. 2009). The specific region of the river analyzed in this study is the Lower Mekong basin located in Cambodia and surrounded by a rectangular region (140 km by 110 km) with Phnom Penh, the capital city of Cambodia, located at its center (Fig. 1). The selected area is located in the tropical zone, and the climate is dominated by two distinct monsoons, the rainy southwest monsoon and the dry northeast monsoon. Annual precipitation averages approximately 1,680 mm across the basin, but shows strong seasonal variations in the lower Mekong, with about 85% of the precipitation occurring during the rainy southwest monsoon season. The southwest monsoon from the Indian Ocean lasts from May to October, while the northeast monsoon from China is active from October to April and brings a dry spell to the basin (Kite 2001; Zhou et al. 2006). During the southwest monsoon period, the basin experiences frequent rainfall. Therefore, the Mekong flood season lasts from July through December with an average discharge of 25,000 m^3/s. The low flow season lasts from January to June with an average discharge of 6,000 m^3/s.

There are two large tributaries in the lower part of the Mekong: the Bassac and Tonle Sap. These rivers join at Phnom Penh, the capital city of Cambodia. The Bassac River flows towards the China Sea, whereas the Tonle Sap River flows from the

Mekong River to the Great Lake (Tonle Sap Lake), which lies in the northern part of the study region and acts as a retention pond for the Mekong. Tonle Sap Lake flows downstream in the dry season, but the flow reverses direction in the rainy season. The lake area is about 3,000 km^2 in the dry season, and it expands to 10,000 km^2 in the rainy season. This is a unique hydrological phenomenon in this region. This area has huge inundation areas that have been expanded by a Colmatage system. Colmatage is a natural irrigation and drainage system that operates through intakes in the dikes along the rivers, according to the flood water level. Farmers use the Colmatage system during the flood season by cutting the levees in flooded areas for irrigation purposes. Flood water flows to the inundation areas through the gaps made in the levee.

2.2. Public health in Cambodia

The population in Cambodia is concentrated in Phnom Penh city, and sanitation and infrastructure development greatly differ between urban and rural areas. This difference is wider than in other Asian countries (WHO 2004). The water quality of the lower Mekong River is similar to other rivers in South East Asia, and it can be used for industrial water after rapid filtration. In Cambodia, diarrheal disease is the second most prevalent disease, affecting 2% of the entire population and 19% of children under 5 years of age (McFeters 1990). In addition, the mortality of children under 5 years, which strongly correlates with sanitation conditions, is the worst among all Southeast Asian countries, with 14% child mortality in Cambodia compared with the mean mortality for Southeast Asia of 4.6% (WHO 2005a).

3. Materials and methods

3.1. Data set

GTOPO30 global elevation model data from the United State Geological Survey (USGS) was used for the numerical simulation. Water level and suspended solid (SS) data were provided by the Mekong River Commission (MRC) (MRC 1995-2002). Cambodian population distribution data and state border data were produced from analog map data made by the Japan International Cooperation Agency (JICA). The coverage of sanitary facilities (water supply and sewage system, pit and digestion tank) and the health index were reported by the Japan Bank of International Cooperation (JBIC 2000). These data are available in digital map format. Daily groundwater level data from the Department of Hydrology, Ministry of Water Resources and Meteorology of Cambodia was also used as input for the numerical model.

Field observations were carried out to collect coliform group counts (CGC) as a measure of the concentration of coliform bacteria and to interview the local people during four different seasons to understand the effects of flood magnitude. We conducted four field observation sessions on October 23, 2004; September 19, 2005; and September 27 and 28, 2006. Coliform bacteria concentration shows significant variations in measurements over the time and spatial extent. Therefore, observations were made in two consecutive days in same places to understand the variation of coliform bacteria concentration over short period of time. However, no significant difference was found between two data sets. We used coliform test papers made by Shibata scientific technology LTD to measure CGCs at 14 points in the inundation area (Fig.1). At each point, three measurements were taken and the data were averaged. The most probable number (MPN) method was also used at four observations time periods to compare the concentration of coliform bacteria with CGC (Fig. 2). There was a good correlation between the two measures. We assumed that the coliform bacteria concentration data in rivers was uniformly 5.0 CFU/ml (APFED 2003). We also measured the concentration of coliform bacteria in Prey Veng city at 17 groundwater well points during the rainy season and 24 points during the dry season. The concentrations in the dry and rainy seasons were almost equal, with a mean value of 367 MPN/100 ml.

The public health center of Kampong Cham province collects daily data on patient outcomes for all diseases. We used patient numbers for diarrhea and dysentery as a measure of waterborne infectious disease. We mainly focused on children under 5 years of age due to their high susceptibility to poor sanitation conditions (WHO 2005a). It is worth noting that this data does not represent actual patient numbers because not all patients visit a health center or hospital when they are sick. However, in this analysis, we assumed that the health center counts did represent all patients.

3.2. Flood modeling

The hydraulic models, which consisted of a dynamic wave model in channels and a non-uniform flow model in inundation areas, were connected by a surge model at Colmatages. Groundwater movement by Darcy’s law and other hydrological processes were also considered. For the simulation of river flooding, the boundary conditions were represented by water level data from Kampong Cham, upstream of the Mekong at Prek Kdam on the Tonle Sap River, and Tan Chau, downstream of the Mekong at Chau Doc on the Bassak River. The integrated model developed by Kazama et al. (2007) showed good agreement between remote sensing data and water level variation after calibration of the model parameters. We used this model to express the advective movements of coliform bacteria.

Suspended solids (SS) were estimated by satisfying the continuity equation such that SS moves with the same concentration at rivers, consistent with the uniform data observed by MRCS. Only deposition is considered, using Rubey's empirical equation:

$$w_f = \sqrt{sgd}\left\{\sqrt{\frac{2}{3}+\frac{36\nu^2}{sgd^3}}-\sqrt{\frac{36\nu^2}{sgd^3}}\right\} \tag{1}$$

where w_f is the sedimentation rate (ms^{-1}), ν is the kinetic viscosity (m^2/s), s (= 1.6687) is the specific gravity of sedimentation in water, and d is the diameter (m). The diameter was obtained by field observations at the Mekong River bank at Phnom Penh by considering the particle size distribution with a passing probability of 80%. From these data, we estimated 4.5×10^{-5} m/s as the sedimentation rate.

3.3. Coliform movement model

During flooding, coliform bacteria from contaminated sources spread into inundation areas via water and sedimentation (Muirhead et al. 2004). The coliform concentration movement was expressed using the discharge calculated from the non-uniform flow model, coliform group load, and survival rate by radiation. Residential areas are the main source of coliform load, as detected by the digital map, and the load amount is estimated from the population and the coverage ratio of sanitary facilities using the following equation.

$$C = n \times c \times (1 - s/100) \tag{2}$$

where C is the coliform group load amount (CFU/day), n is the population (persons), c

is the individual coliform group load amount ($= 2.0 \times 10^{10}$ CFU/person/day) (Kaneko 1997), and s is the coverage ratio of sanitary facilities in each province.

The survival rate per hour is determined mainly by the water temperature, solar radiation, and other bacteria (MacFeters 1990; Gameson and Saxon 1967). Downstream of the Mekong, the temperature is almost constant throughout the year and does not greatly affect the survival rate. On the other hand, solar radiation in tropical regions does strongly affect the survival rate. Therefore, we estimate the survival rate of coliforms from solar radiation using the relationship between the net cumulative radiation and water depth (Gameson and Saxon 1967). We developed a formula to estimate the survival rate from Gameson and Saxon’s results, as shown in Figure 3. In addition, the net cumulative radiation was evaluated by considering the reflection of downward radiation on the water surface due to the SS concentration using the following equation:

$$S = (1 - R/100)S_{\max} \quad (3)$$

where S is the net cumulative solar radiation (J/cm^2/day), S_{max} is the downward solar radiation (J/cm^2/day), and R is the reflection (%).

Oki et al. (2001) used the following function to explain the relationship between SS concentration and reflection:

$$R = 0.0809 + 0.0146U \quad (4)$$

where U is the SS concentration (mg/l), as calculated by the hydraulic simulation considering sediment movement. We can evaluate the temporal and spatial distribution of coliform group counts using the hydraulic model-like SS estimation for the advection and the coliform movement model, consisting of the above equations, for the survival rate.

3.4. Risk evaluation

To evaluate the attributed risk, we used the dose-response model, which indicates the probability of infection for a given exposure amount according to the single-hit hypothesis. The dose-infection model is based on the following function:

$$R_Y = 1 - (1 - P(D))^{365} \tag{5}$$

where R_Y is the probability of infection of a host that is infected once for one year and *P(D)* is the probability of infection for one exposure, depending on exposure amount *D*, which is expressed by equation (6) based on the Beta-Poisson formula:

$$P(D) = 1 - \left[1 + \frac{D}{\beta}\right]^{-\alpha} \tag{6}$$

where α and β are empirical parameters that depend on the pathogen. Here we used α = 0.1778 and $\beta = 1.78 \times 10^6$ for *E. coli* (Rose et al. 1999). We assumed that daily water drinking water volume was 2 liters, and the exposure level in the inundation area and groundwater were estimated by the coliform movement model to be 367 MPN/100 ml, the mean value of the field survey. The conversion rate of CGC in MPN experiments with *E. Coli* was determined by the relationship observed in field surveys (Fig. 2) (Gronwold and Wolpert 2008).

Considering seasonal changes in water resources, we assume that residents use surface water if the flood model shows inundation, and groundwater otherwise. We used a constant value for the *E. coli* in groundwater which was recorded from field observations (367MPN/100ml). Here, we assumed that *E. coli* can be expressed by the concentration of coliform bacteria.

4. Results and Discussion

4.1. Spatial distribution of coliform concentration

Figure 4 shows the simulated and observed concentrations of coliform bacteria measured by test papers at the sampling points during the rainy season. Each data point represents the average of the measured values from four observations (average of the measured concentrations of coliform bacteria from October 23, 2004; September 19, 2005; and September 27 and 28, 2006). The simulated data was from the end of September 2000. Although the observed and simulated results were not from the same date, the process and phenomena were similar across different years, which will be important for helping us to understand the relative risk distribution attributed to different sources in the study area. Figure 4 shows that the observed values at sampling points 4 and 10 were much higher than the simulated results. The reason for these differences is that point 4 has a higher population than that used to produce the digital data, and point 10 is close to an irrigation pond and is full of water during the entire season. With the exception of these two cases, the observations were in good agreement with the simulated results.

4.2. Provincial risk assessment

When we consider using CGC for risk assessment, the contact opportunity should be evaluated as well as the concentration. The contact opportunity can be substituted with the inundation period, but the coliform concentration is not correlated with the inundation period. Here, the annual integrated concentration is used for the risk assessment according to the following equation:

$$\overline{E} = \int_{t=1year} E\,dt \qquad (7)$$

where E is the simulated CGC and $\overline{E}$ is the annual integrated CGC. The annual integrated CGC represents the sum of the concentrations of coliform bacteria with which the residents in a calculation area come into contact over the course of a year. We assumed that a larger concentration means a higher risk.

Figure 5 shows the correlation between the annual integrated CGC simulated for a year and the mortality rate for children under 5 years of age in 3 provinces within inundation areas. It clearly shows that mortality increases with coliform concentration. Using this result, we can conclude that the concentration of coliform bacteria can be used as a risk index for waterborne infectious diseases.

4.3. Distribution of risk assessment

The dose-response model coupled with the hydraulic model can estimate the spatial and temporal distribution of the probability R_Y of infection of a host as the risk of waterborne infectious disease. Figure 6 shows the distribution of the annual risk in the case of a small flood (in 1998), a medium-sized flood, (in 1993), and a large flood (in 2000).

Figure 7 depicts the distribution of the risk of surface water use in inundation areas. Rural communities experience low risk (0.02-0.06), where as high-risk areas exist in urban and residential areas with a mean risk of 0.70. This is much higher risk, but most urban residences use bottled mineral water for drinking. The high-risk area pattern differs by flood magnitude. Figure 7 clearly shows that there are no areas of concentrated high risk during a large flood. Large floods spread the concentration of coliform bacteria further from the source point and dilute the concentration. Nevertheless, residential areas still have a high risk of infection.

Figure 8 shows the distribution of the risk of groundwater use in the dry areas, using the hydraulic simulation results. Rural communities living in hilly regions surrounded by inundation areas use groundwater for their daily needs. Field observations recorded the risk of infectious diseases for one year in the whole area as 0.23. This is significantly greater than the infection risk due to the surface water (0.02-0.06) in the region outside the inundation area. People in inundation areas use groundwater after the inundation retreats. After the inundation, groundwater may accumulate a lot of pollutants and may be contaminated with infectious pathogens. According to Figures 7 and 8, the infection risk attributed to groundwater (0.12-0.17) in inundation areas is still higher than the risk due to surface water use (0.02-0.06), except in largely populated areas.

4.4. Infection risk and water sources

The simulations explain the diffusion processes that cause large discharges to bring the risk of infectious disease to places further away, in terms of annual average risk and the risk due to surface water use. The locations that are high risk due to surface water use are closer to densely populated areas and near the border of inundation areas; these areas exposed to risk independent of the flood magnitude. Remote areas where people use groundwater throughout the year have a constant risk of 0.23. According to Figure 6, a medium-sized flood produces new and wider risk areas in the southeast region. This means that some record-breaking floods produce new risk areas where people have not had experience dealing with waterborne infectious diseases. These kinds of places are vulnerable for spreading diseases.

Table 1 show the summary of the estimated risk, depending on the flood magnitude and water use. Small floods lead to a subsequent dry period in remote areas and the risk from groundwater wells increases in those areas because of the increase in groundwater use. The infection risk due to surface water use increases as the flood magnitude increases and become stable once the flood magnitude reaches middle-size. Due to the significantly higher risk of surface water use in highly populated areas (0.610-0.937), mean annual risk in the whole area attributed to surface water use show slightly higher values than the risk attributed to groundwater use (Table 1). However, the resultant risks in suburban and rural areas due to groundwater use are comparatively higher than the risks of surface water use. The mean annual risk in residential areas becomes very high (0.94) during small flood events. On the other hand, the annual average risk in and around residential areas decreases as the flood magnitude increases because shallow water has high concentrations of coliform due to storing and enrichment. During the dry season, we can see many isolated ponds in the inundation areas and a lot of people enjoy swimming and bathing in these ponds. The infection risk exists not only in drinking water, but also due to contact with contaminated water (Geldreich 1998).

4.5. Reduce the risk using countermeasures

The reason for the high risk of infection in residential areas is that the surface water is polluted with high concentrations of coliforms when the water level is lower. Figure 9 depicts the relationship between the annual average risk in the residential areas and the surface water level (the safe water level). Each flood scale has a rapid decrease in risk until the water level reaches 0.3 m and then the rate of reduction is less as the water level continues to increase. In the case of a small flood, the risk does not go below 0.5, even when the water level for safe surface water use is 2.0 m. Although the local people prefer to use groundwater during the dry season, the Cambodian groundwater is contaminated with arsenic in many places, and the risk is too high (Feldman et al. 2007). Therefore, one countermeasure to prevent infection is to restrict the people to using surface water during the low water level season, once the water falls below a certain level (e.g. 0.3 m in Figure 9). This countermeasure can reduce 50% of the risk and is a very effective method. In practice, people particularly in high risk areas (but not restricted to) must be advised to use household water treatment methods like boiling to treat the infected water before drinking. Moreover, a simple and cost-effective method like solar disinfection can be promoted by public campaigns.

One of the other problems causing the high risk of infection in residential areas is that the water sources are located closer to garbage dumping sites. Therefore, separation of the water sources from infection sources, such as garbage disposal sites and septic tanks, is another potential countermeasure for reducing the risk of waterborne infectious diseases. Moreover, changing the structure of drainage and irrigation channels to remove stagnant water from storage ponds also reduces the risk. It is not only measures affecting the infrastructure, but also “software” measures, such as health programs, that are effective for reducing the infection risk (Courtney 2007). The simulated results in our study explain the spatial distributions of infection risk attributed to different sources (e.g., surface water and groundwater) in different geographical settings (e.g., urban, suburban and rural areas). Such distribution maps for risk are vitally important for determining the highest priority places with relatively high risk and will be helpful for decision makers when considering the implementation of countermeasures.

5. Conclusions

This study developed models to evaluate the risk of waterborne infectious disease in inundation areas in a developing country, Cambodia. The model combined hydraulic, hydrologic, and dose-response models. The model parameters were calibrated using field survey data in Cambodia and obtained good agreement with the CGC distribution. The annual average risk in the study area is 0.21, in the case of a medium-scale flood. The risk of groundwater use is 0.12-0.17 in inundation areas and as high as 0.23 outside the inundation areas. The risk attributed to groundwater use is therefore higher than that due to surface water use (0.02-0.06), except in densely populated areas at the city center. There is a high risk of infection with waterborne disease in residential areas, and the annual average risk during small flood events is as high as 0.94. The annual average risk around residential areas decreases as the flood magnitude increases because shallow water has a higher concentration of coliform due to storing and enrichment. Qualitatively, the reduction of flood scale increases the infection risk. An assessment of possible countermeasures to reduce the risk shows that restricting surface water use in residential areas, except in low water level seasons (< 0.3m), may increase public health risks in Cambodia. This macro-scale analysis will be useful for making decisions regarding countermeasures for reducing the risk of infection. In practice, linkage between macro- and micro- scale countermeasures will be needed to protect the public health in inundation areas.

Acknowledgements

This study was made possible largely through Grants-in-Aid for Scientific Research from the Japan Society for the Promotion of Science (JSPS) (Category B) and through a grant from the integrated research system for sustainability science (IR3S). We would like to acknowledge here the generosity of these organizations. We also wish to thank Dr. Hong Rathmony and Dr. Duong Socheat from the Ministry of Health in Cambodia and Dr. Satoshi Nakamura at the International Medical Center of Japan for their generous assistance with the field investigations.

References

APFED (2003) the Asia-Pacific Forum for Environment and Development report, 0 draft.

Courtney J (2007) Dose partnership and sustainability really happen? A case study of an in-service health education programme implemented in one province in Cambodia. Int. J. Educational Development 27: 625-636

Curriero FC, Pats JA, Rose JB, Lele S (2001) The association between extreme precipitation and waterborne disease outbreaks in the United States, 1948-1994. Am. J. Public Health 91: 1194-1199.

Feldman RR, Rosenboom J, Saray M, Samnang C, Navuth P, Iddings S (2007) Assessment of the chemical quality of drinking water in Cambodia. J. Water and Health 5: 101-116.

Gameson ALH, Saxon JR (1967) Field studies on effect of daylight on mortality of coliform bacteria. Water Research 1: 279-295

Geldreich EE (1998) Pathogenic agents in freshwater resources. Hydrol. Processes 10:

315-333

Gronewold, A.D., Wolpert, R.L. 2008. Modeling the relationship between most probable number (MPN) and colony-forming unit (CFU) estimates of fecal coliform concentration, Water Research, 42, 3327-3334.

Haines A, Kovats RS, Campbell-Lendrum D, Corvalan C (2006) Climate change and human health: impacts, vulnerability and public health. Public Health 120: 585-596

Herath, S., Dutta, D., (Ed.), 2000. Mekong Basin Studies, Proceedings of the AP FRIEND Workshop, INCEDE Report 19, University of Tokyo, Japan.

Hunter PR, Colford JM, LeChevallier MW, Binder S, Berger PS (2001) Waterborne disease. Emerging Infectious Diseases 7: 544-545.

Huu-toi, N., Das Gupta, A., 2001. Assessment of water resources and salinity intrusion in the Mekong delta, IWRA. Water International 26 (1), 86–96.

Inoue, K., Toda, K., Maeda, O., 2000. A mathematical model of overland inundating flow in the Mekong Delta in Vietnam. Ecosystem and flood, unpublished report.

JBIC (2000) Poverty Profile, Kingdom of Cambodia Poverty profile (in Japanese).

Kaneko M (1997) Antisepsis of water, Japan Education Center Environmental Sanitation (in Japanese)

Kazama S, Hagiwara T, Ranjan P, Sawamoto M (2007) Evaluation of groundwater resources in wide inundation areas of the Mekong River basin. Journal of Hydrology 340: 233-243

Kazama S, Morisugi H, Sawamoto M (2003) Integrated evaluation of the Mekong River flood using benefit calculation. J. Hydroscience and Hydraulic Engineering, JSCE 21:

85-92

Kite G (2001) Modeling the Mekong: hydrological simulation for environmental impact studies. Journal of Hydrology 253: 1-13

Kunii O, Nakamura S, Abdur R, Wakai S (2002) The impact on health and risk factors of the diarrhoea epidemics in the 1998 Bangladesh floods. Public Health 116: 68-74

Liu S., Lu P., Liu D., Jin P., and Wang W., 2009. Pinpointing source and measuring the lengths of the principal rivers of the world. International Journal of Digital Earth, 2, 80-87.

Lloyd BJ, Bartram JK (1991) Surveillance solutions to microbiological problems in water quality control in developing countries. Water Science & Technology 24: 61-75

Lopez-Pila JM, Szewzyk R (2000) Estimating the infection risk in recreational waters from the faecal indicator concentration and from the ratio between pathogens and indicators. Water Res. 34: 4195-4200

McFeters, G.A., 1990. Drinking Water Microbiology, Springer-Verlag Berlin and Heidelberg GmbH & Co.

MRC (1995-2002) Lower Mekong Hydrologic yearbook.

Muirhead RW, Davies-Colley RJ, Donnison AM, Nagels JW (2004) Faecal bacteria yields in artificial flood events: quantifying in-stream stores. Water Research 38: 1215-1224

Oki K, Yasuoka Y, Tamura M (2001) Estimation of Chlorophyll-a and Suspended Solids Concentration in Rich Concentration Water Area with Remote Sensing Technique. Journal of the Remote Sensing Society of Japan 21: 449-457

Rose JB, Daescner S, Easterling DR, Curriero FC, Lele S, Pats J (2000) Climate and waterborne disease outbreaks. J. AWWA 92: 77-87

Rose JB, Haas CN, Gerba CP (1999) Quantitative Microbial Risk Assessment. John Wiley & Sons.

Schwartz, B.S., Harris, J.B., Khan, A.I., Larocque, R.C., Sack, D.A., Malek, M.A., Faruque, A.S.G., Qadri, F., Calderwood, S.B., Luby, S.P., Ryan, E.T., 2006. Diarrheal epidemics in Dhaka, Bangladesh, during three consecutive floods: 1988, 1998, and 2004. Am. J. Tropical Medicine and Hygiene. 74, 1067-1073.

Smith E (2001) Pollutant concentrations of stormwater and captured sediment in flood control sumps draining an urban watershed. Water Res. 35: 3117-3126

WHO (2000) Global water supply and sanitation assessment 2000 report. (http://www.who.int/water_sanitation_health/monitoring/globalassess/en/)

WHO (2004) Country Health Information Profile 2004 (http://www.wpro.who.int/chips)

WHO (2005a) The World Health Report 2005

WHO (2005b) Weekly epidemiological record. 3: 21-28

Zhou MC, Ishidaira H, Hapuarachchi HP, Magome J, Kiem AS, Takeuchi K (2006) Estimating potential evapotranspiration using the Shuttleworth-Wallace model and NOAA-AVHRR NDVI data to feed a distributed hydrological model over the Mekong river basin. Journal of Hydrology 327: 151-173

Figure captions

Figure 1 – (a) The study area in Cambodia and (b) the sampling locations for the coliform group counts.

Figure 2 – The correlation of the concentration of coliform bacteria (*E. coli*) with CGC.

Figure 3 – The relationship between the mortality ratio of coliforms and net cumulative solar radiation (an Improvement on the results by Gameson and Saxon 1967).

Figure 4 – A comparison between the observed and simulated concentrations of coliform bacteria.

Figure 5 – The relationship between the annual integrated CGC and the annual infant mortality rate in each province.

Figure 6 – The annual infection risk, depending on flood magnitude.

Figure 7 – The infection risk due to surface water use, depending on flood magnitude.

Figure 8 – The infection risk due to groundwater use, depending on flood magnitude.

Figure 9 – The average annual infection risk in residential areas and the water level of surface water use restrictions.

1.

b)

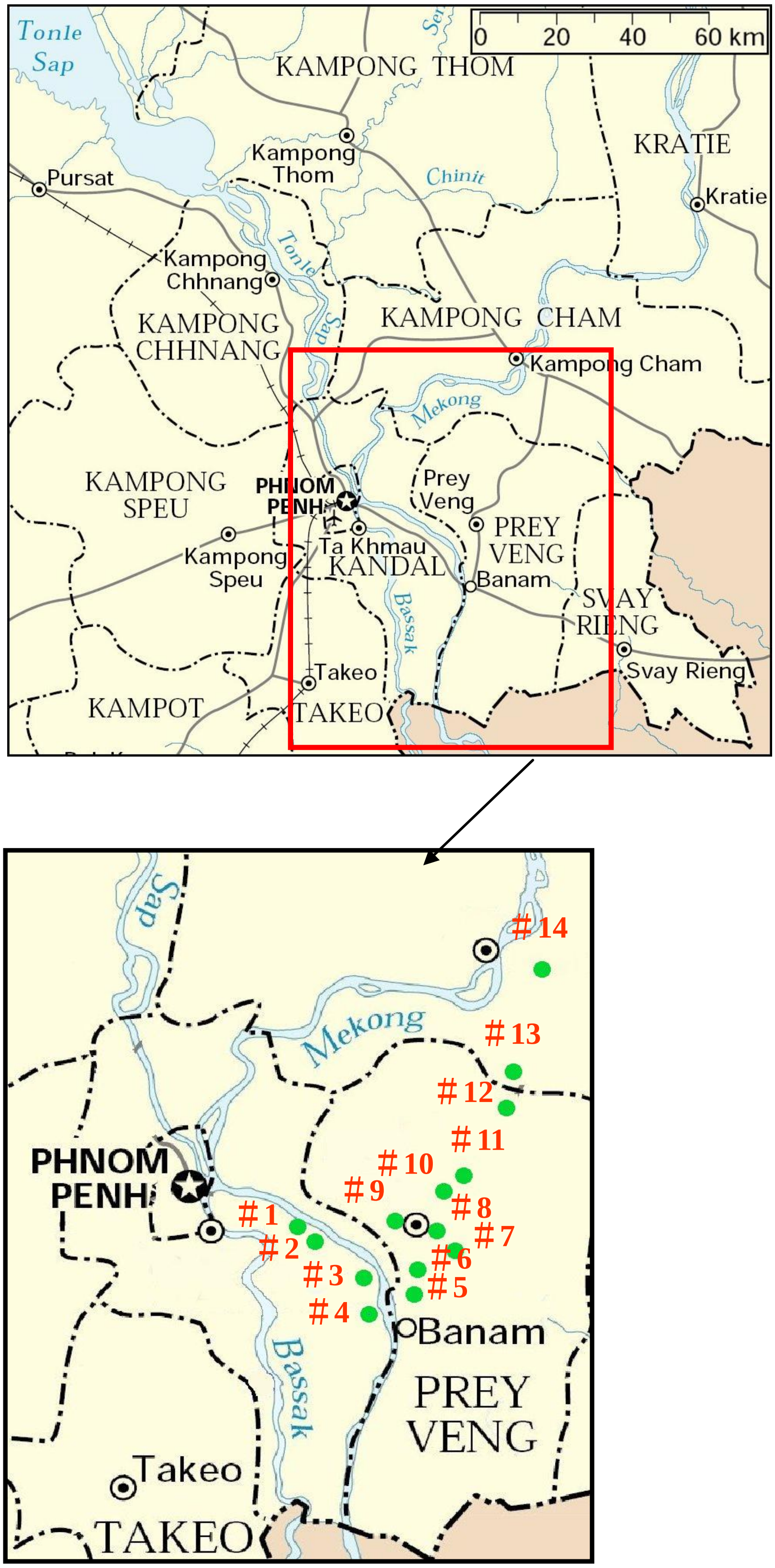

Fig. 1 (a) The study area in Cambodia and (b) the sampling locations for the coliform group counts

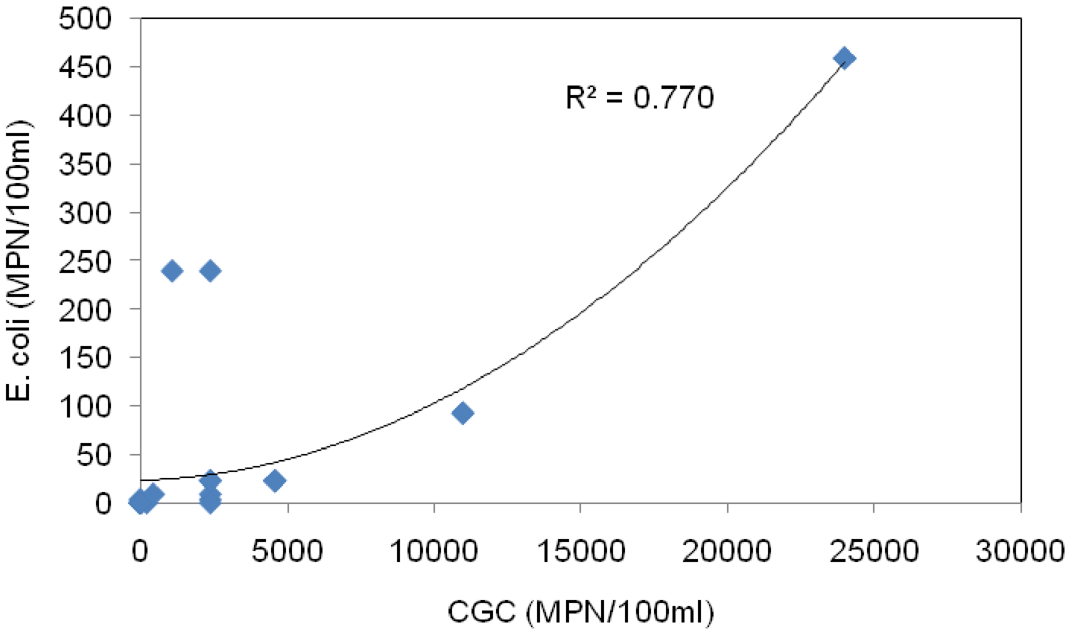

Fig. 2 The correlation of the concentration of coliform bacteria (*E. coli*) with CGC

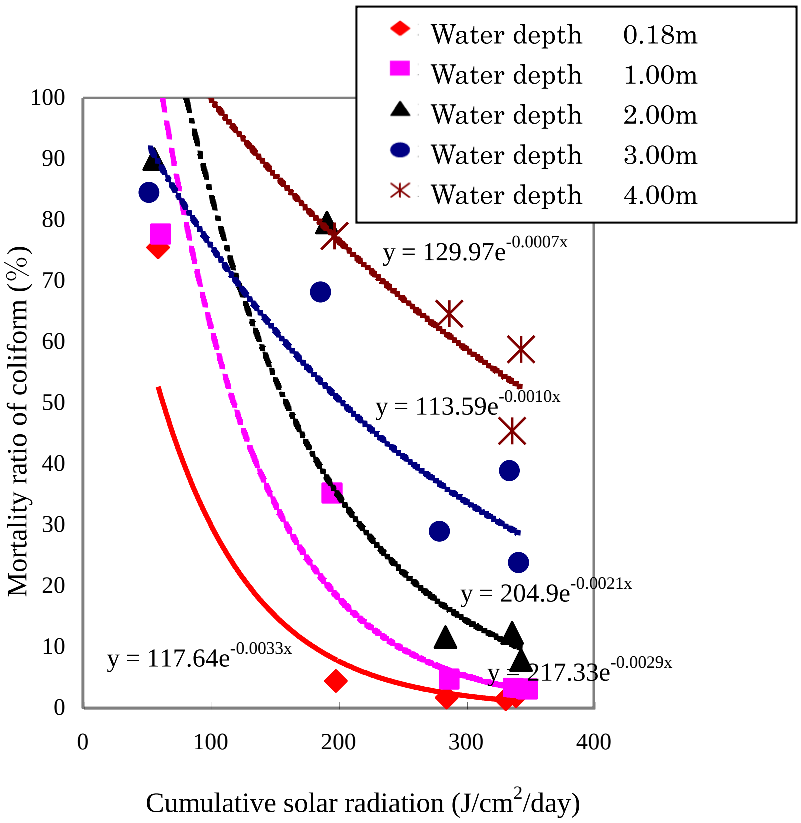

Fig. 3 The relationship between the mortality ratio of coliforms and net cumulative solar radiation (an Improvement on the results by Gameson and Saxon 1967)

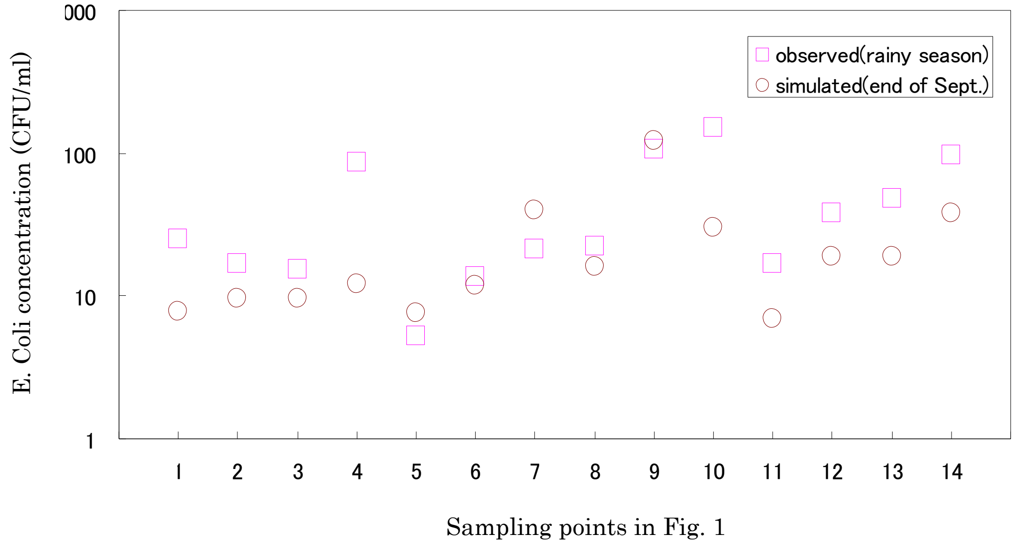

Fig. 4 A comparison between the observed and simulated concentrations of coliform bacteria

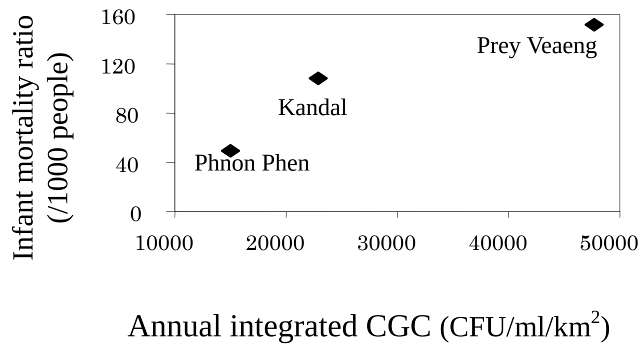

Fig. 5 The relationship between the annual integrated CGC and the annual infant mortality rate in each province

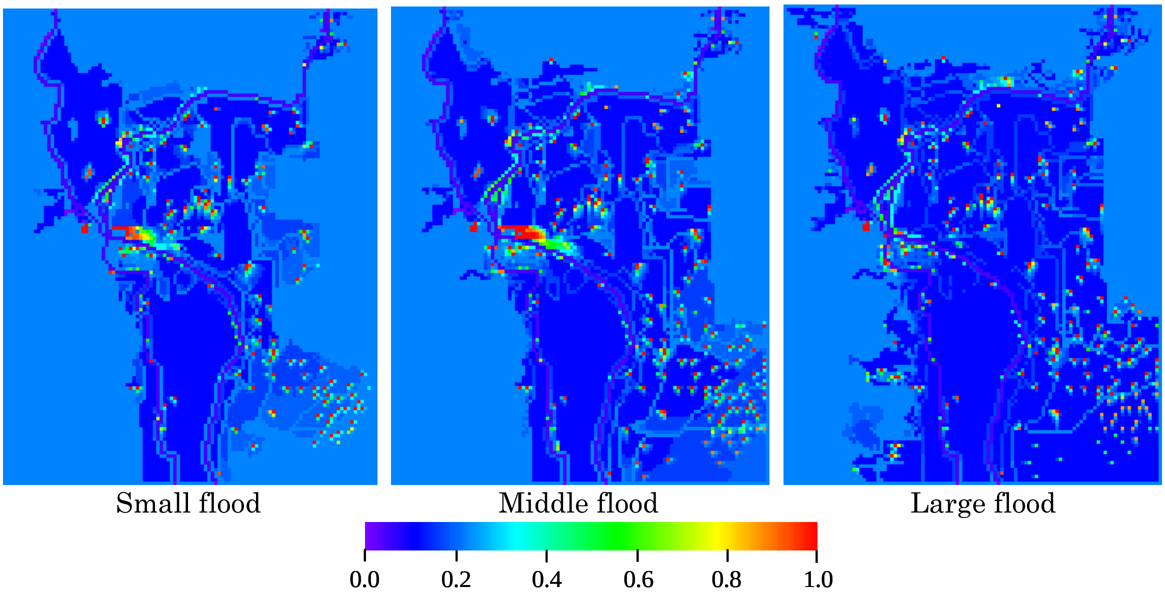

Fig. 6 The annual infection risk, depending on flood magnitude

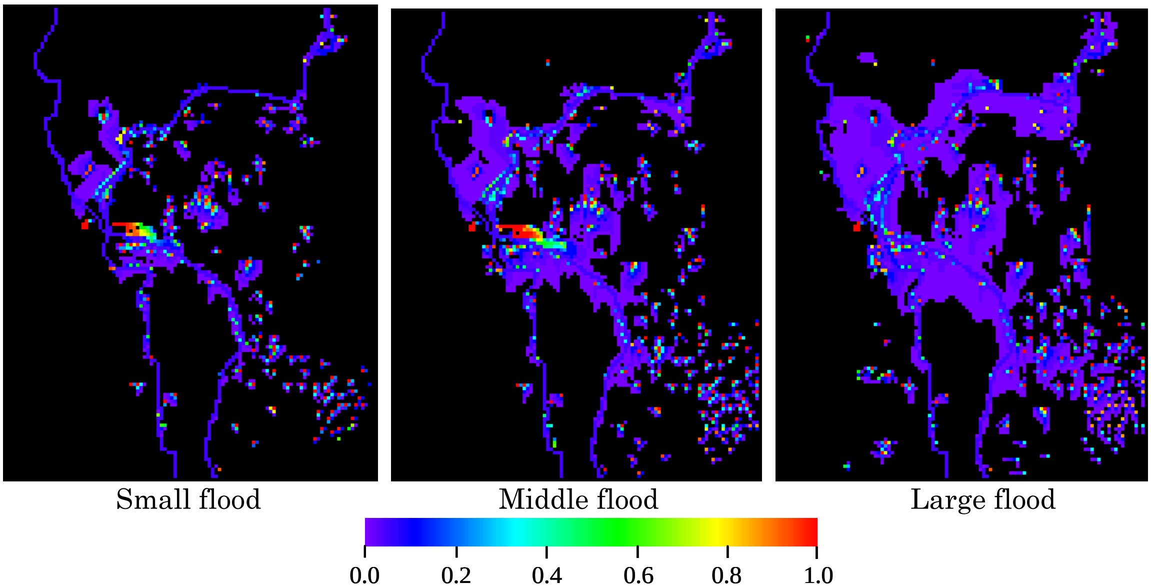

Fig. 7 The infection risk due to surface water use, depending on flood magnitude

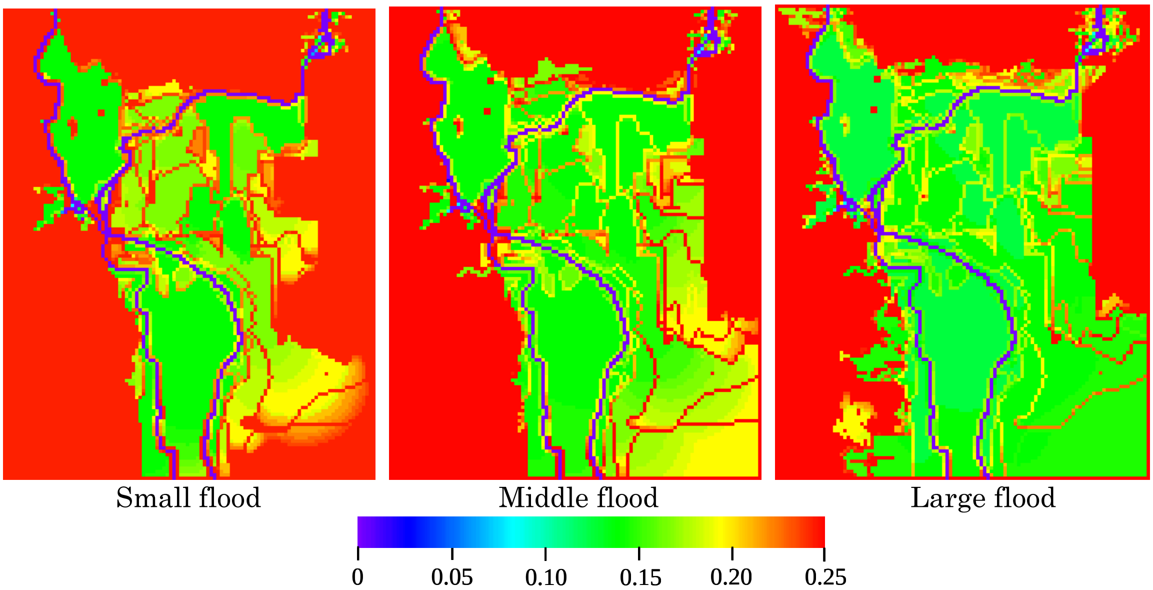

Fig. 8 The infection risk due to groundwater use, depending on flood magnitude

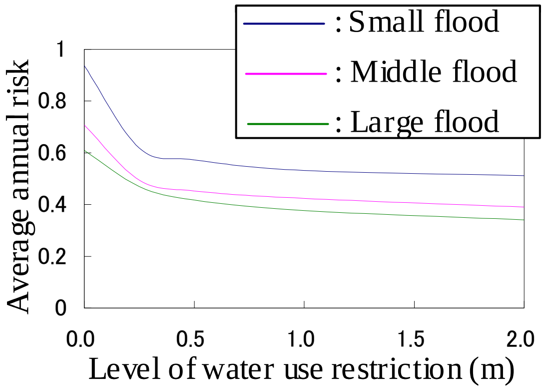

Fig. 9 The average annual infection risk in residential areas and the water level of surface water use restrictions

Table 1- The estimated risk, depending on the flood magnitude and water use

	Mean annual risk in the whole area	Groundwater use period	Surface water use period	Mean annual risk in residential areas
Small flood	0.215	0.198	0.020	0.937
Middle flood	0.210	0.187	0.026	0.707
Large flood	0.179	0.171	0.026	0.610